Journal of Engineering Science and Technology
Vol. 13, No. 6 (2018) 1793 - 1804

HYDRODYNAMIC AND HEAT TRANSFER STUDIES IN RISER SYSTEM FOR WASTE HEAT RECOVERY USING LIMESTONE

A. K. POPURI[1,2,*], P. GARIMELLA[1]

[1]Department of Chemical Engineering, S. V. U. College of Engineering,
S. V. University, Tirupati, Dist.: Chittoor, Andhra Pradesh, India
[2]Department of Chemical Engineering, VFSTR,
Vadlamudi, Dist.: Guntur, Andhra Pradesh, India
*Corresponding Author: akpopuri@gmail.com

Abstract

Suspension pre-heater (SP) system has been a unique development in the field of cement manufacture. A modern dry process cement plant vitally constitutes, the suspension pre-heater and the pre-calcinator, which together account for a drastic reduction in the specific energy consumption in the klin, to as low as800 kcal/kg clinker. Experimental investigations were carried out using limestone particles in a metallic fluid particle heat exchanger. Acceleration length is determined by plotting pressure gradient versus riser height. From the model, experimental gas and solid temperatures were measured at different heights of the riser. Exhaustive heat transfer studies were made in hot model by varying particle size, solid flow rate and gas velocities. An empirical correlation is developed for the Nusselt number using regression analysis.

Keywords: Acceleration length, Gas velocity, Particle size, Solid loading ratio, Suspension preheater system.

1. Introduction

Suspension pre-heater system has been a unique development in the field of cement manufacture [1]. The first patent concerning raw mix suspension pre-heater was applied for by M. Vogel Jorgenson and submitted to the patent office in Czechoslovakia and the technology was implemented [2, 3]. Subsequent modifications have emerged all over the world with various designs of SP system [4, 5]. Four to five cyclones are usually arranged in stages, one above the other and connected by long vertical gas ducts [6]. The cement raw mix (limestone, clay and bauxite) is introduced in the transporting system leading to the top cyclone (first stage) and thereby gets preheated in the suspended state by means of the uprising

Nomenclatures

D_p	Particle size, µm
L	Length of riser, m
L_A	Acceleration length, m
Nu	Nusselt number
Pr	Prandtl number
Re_p	Particle Reynolds number
t_g	Gas temperature, ^oC
t_p	Solid temperature, ^oC
u_g	Gas velocity, m/s
W_g	Gas federate, kg/s
W_s	Solid federate, kg/s

Greek Symbols

ΔP	Pressure drop, Pa
ρ_p	Particle density, kg/m^3

hot gas coming from the second cyclone [7, 8]. The suspension then enters the first cyclone for separation of solids from the gaseous stream [9, 10]. The down coming, partially heated particles enter the interconnecting gas duct between the second and third stage, where the hot gas ascending from the third stage cyclone, preheats the particles in a similar manner. In this way, the solids get preheated to the desired temperature, thereby resulting in high heat recovery from the kiln gas [11, 12].

The objectives of the present study are, fabrication of an experimental apparatus to study exhaustive hydrodynamic and heat transfer aspects by varying type of material and its size, solid feed rate and fluid velocity, formulation of an empirical model for the riser hydrodynamic studies and prediction of the acceleration (or mixing) length (L_A), study the variation of acceleration length with different parameters viz. fluid velocity, particle size, solid loading ratio, material density, exhaustive heat transfer studies in hot model by varying particle size, solid flow rate and gas velocities, measurement of instantaneous gas and particle temperatures along the riser and determination of rate of heat transfer, overall heat transfer coefficients at different solid feed rates and gas flow rates and development of an empirical correlation for Nusselt number as function of Reynolds and Prandtl numbers using regression analysis.

2. Experimental Aspects

Studies on hydrodynamic behaviour and heat transfer characteristics of the riser were carried out using cold and hot model experimental setup for sand-gas, limestone-gas and chalcopyrite-gas systems.

2.1. Experimental setup

Schematic diagram and fabricated experimental set-ups are shown in Figs. 1 and 2. The set-up essentially consists of a vertical transport duct (*A)*, cyclone Separator (*B*), solid storage tank (*C*), standpipe (*D*), solid feeding line (*E*), bend (*F)*, orifice meter (*G*), blower (*H*), solid collection pot (*I*), auxiliary gas inlet (*J*), electric furnace (*K*), all made up of steel.

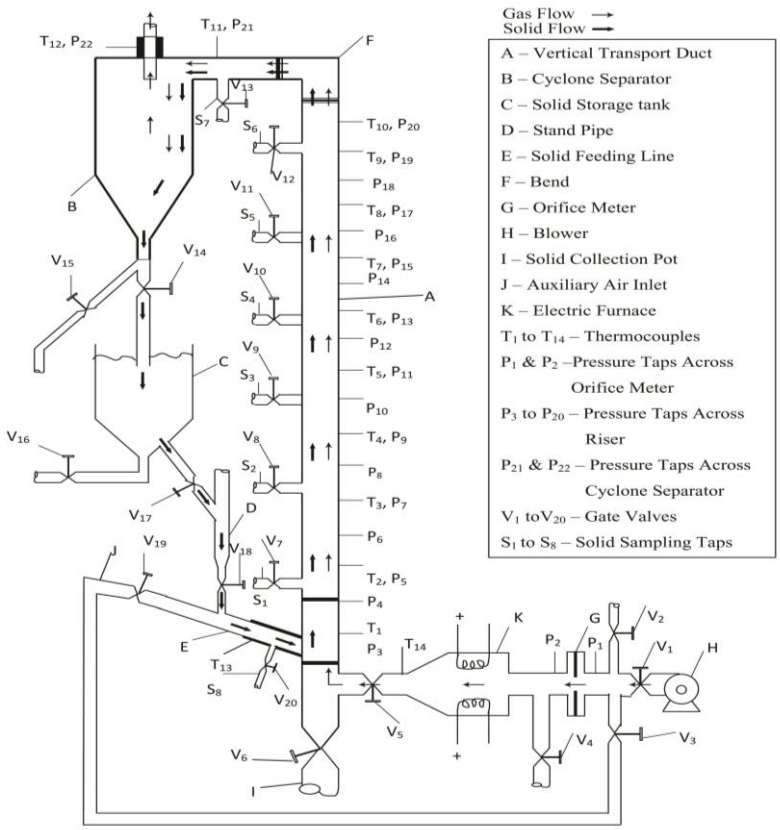

Fig. 1. Schematic diagram of experimental setup.

Fig. 2. Fabricated experimental setup.

2.2. Experimental procedure

2.2.1. Hydrodynamic studies

The desired material of predetermined size (98 to 480 μm) is charged into the storage tank and the rotary valve is adjusted for the specific solid feed rate. Gas from the blower is metered and then sent through the bottom of the riser to transport the solids vertically upward. The solids gets separated in the cyclone separator, travels along the down comer and recycled into the storage vessel. Provision has been made for the collection of solid samples. Introduction of auxiliary gas helps in the aeration, there by resisting choking tendency, if any. The static pressures along the riser height are measured with the help of water manometers after the system reaches steady state. The differential pressure can be found across any section of the riser. The pressure drop in the cyclone is also measured. Similar readings are taken by varying the size (98 to 480 μm), type of the material (sand, limestone and chalcopyrite), the solid feed rate (0.011 to 0.041 kg/s) and the gas velocity (6.6 to 15.3 m/s).

2.2.2. Heat transfer studies

The desired material of predetermined size is charged into the storage tank and the rotary valve is adjusted for a specific solid feed rate. Gas from the blower is preheated to the desired temperature in the electric furnace. As the hot gas moves upwards, the solid is fed into the riser, which behaves as a parallel flow heat exchanger. The gas velocity is so maintained as to ensure pneumatic transport of the solid particles. As recorded by the thermocouples, the gas temperature gradually decreases. As a result of the interchange of heat, the particle temperature steadily increases. At steady state, solid samples are collected from various points into the stand-by calorimeters. The final temperatures attained by the mercury thermometers in the calorimeters are recorded to find the temperature profile of solid within the riser. In a similar manner, data on variations in gas and particle temperatures are taken at different gas velocities and solid feed rates. Other parameters include the size of material and temperatures of the incoming hot gas are studied.

3. Results and Discussion

3.1. Hydrodynamic studies-acceleration (or mixing) length

Starting from the injection of material into the duct, various forces act upon the particles. Depending upon the mode of injection, the particle can be either at zero or at negligible velocity, after which it steadily increases at the expense of the kinetic energy of the fluid. At a certain riser height, the particle velocity reaches a maximum value, which evidently depends on the system conditions. Once this velocity is reached, the particles will behave as a homogeneous (dispersed) gas-solid suspension. This minimum length (or height) required for ensuring a steady homogeneous flow, has been termed as the "Acceleration Length", L_A or "Entry Length" or "Mixing Length".

By plotting static pressure distribution against the riser height, an asymptotic trend is observed. When a cross plot is made with the pressure drop per unit length (or height) as the ordinate and the riser height as the abscissa, it is observed that at

a certain point, irrespective of the increase in the riser height, the pressure drop per unit length (or height) remains substantially constant. This particular length (or height) gives the desired value after which a homogeneous suspension flow occurs. Using the below equation, values of pressure gradient $\Delta P/\Delta L$ at different riser heights were found using Eq. (1).

$$[\Delta P/\Delta L]_{ito(i+1)} = \left[\Delta P_{(i+1)to0} - \Delta P_{ito0}\right]/\left[L_{(i+1)to0} - L_{ito0}\right] \quad (1)$$

3.1.1. Effect of gas velocity on acceleration length

Observing the values in Table 1 and Fig. 3, one can infer that the acceleration length increases with an increase in the superficial velocity of the gas. This is possibly due to the fact, that at high gas velocity, the particle velocity increases because of enhanced momentum transfer and so, the particle has to travel a longer distance before the steady state can be attained.

Table 1. Variation of acceleration length with gas velocity. (Particle size: 98 μm; Solid feed rate: 0.018 kg/s)

Gas Velocity (u_g), m/s	Acceleration Length (L_A), m
6.6	0.6
8.1	0.8
14.6	1.2

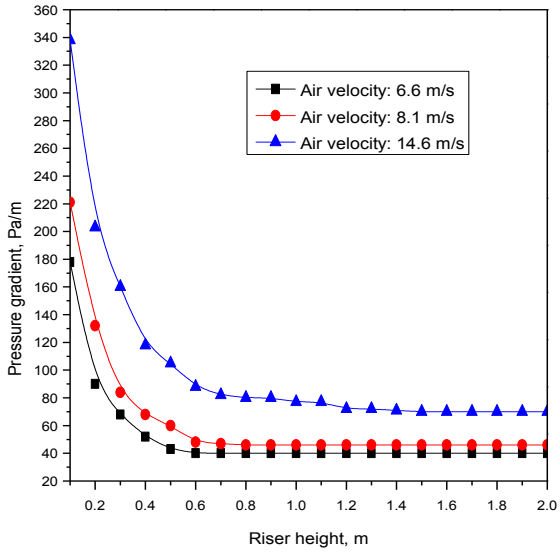

Fig. 3. Variation of pressure gradient along riser height with gas velocity. (Particle size: 98 μm; Solid feed rate: 0.018 kg/s)

3.1.2. Effect of particle size on acceleration length

It can be inferred from Table 2 and Fig. 4 that it is exhibiting a general trend, indicating that the acceleration length increases with an increase in the particle size. This is due to, higher particle size demands higher acceleration length, indicating

the difficulty in accelerating bigger particles to a velocity equal to the gas velocity, overcoming the forces of gravity and drag.

Table 2. Variation of acceleration length with particle size. (Gas velocity: 15.3 m/s; Solid feed rate: 0.0133 kg/s)

Particle Size (d_P), μm	Acceleration Length (L_A), m
98	1.0
240	1.1
480	1.3

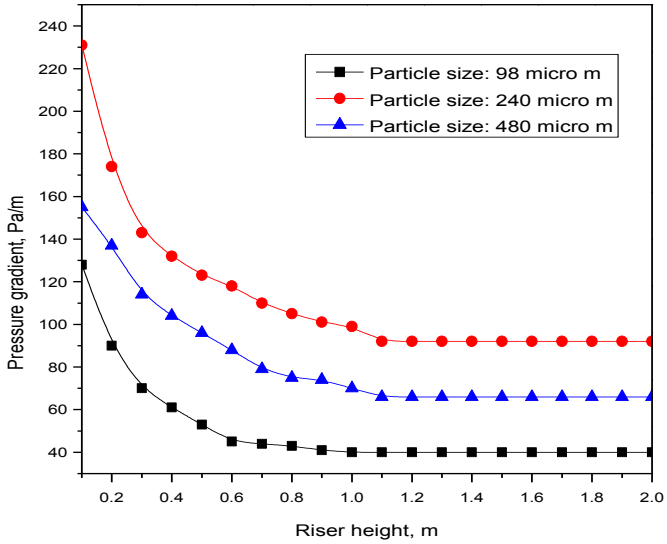

Fig. 4. Variation of pressure gradient along riser height with particle size. (System: Limestone-Gas; Gas velocity: 15.3 m/s; Solid feed rate: 0.0133 kg/s)

3.1.3. Effect of solid feed rate on acceleration length

By observing Table 3 and Fig. 5, one can infer that, for a set of conditions, the accelerating length decreases with an increase in the solid feed rate. This can be explained by the fact that an enhanced solid flux reduces the void fraction, thereby resulting in higher interstitial velocity, which enhances the drag on the particle and thus reduces the length of the riser necessary to attain a stable flow condition.

Table 3. Variation of acceleration length with solid feed rate. (Gas velocity: 10.64 m/s; Particle size: 98 μm)

Solid Feed Rate (w_S), kg/s	Acceleration Length (L_A), m
0.011	0.9
0.018	0.8
0.041	0.7

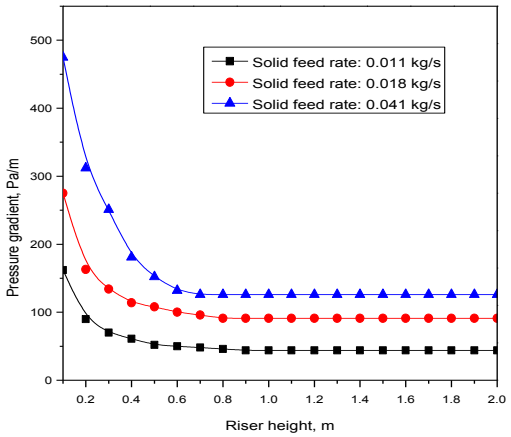

Fig. 5. Variation of pressure gradient along riser height with solid feed rate. (Gas velocity: 10.64 m/s; Particle size: 98 μm)

3.1.4. Effect of material density on acceleration length

It can be inferred from Table 4 and Fig. 6 that an increase in the material density enhances the accelerating length when all other parameters remain constant. This may be because of an increase in the gravitational force and corresponding in the drag.

Table 4. Variation of acceleration length with material density. (Gas velocity: 14.66 m/s; Solid feed rate: 0.0376 kg/s; Particle size: 98 μm)

Material Density (ρ_p), kg/m^3	Acceleration Length (L_A), m
2640	0.9
2730	1.0
3130	1.1

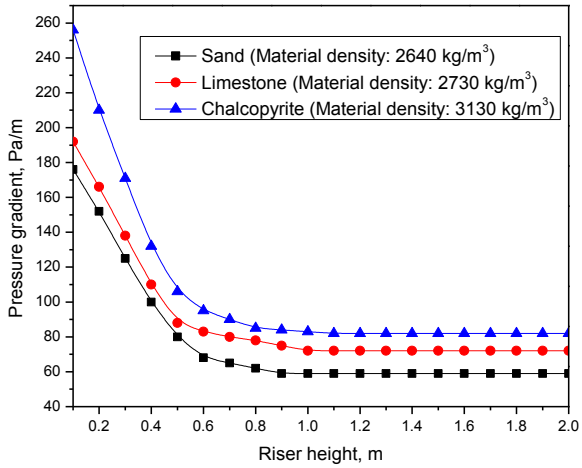

Fig. 6. Variation of pressure gradient along riser height with material density. (Gas velocity: 14.66 m/s; Solid feed rate: 0.0376 kg/s; Particle size: 98 μm)

Through regression analysis of the experimental data, the regression coefficient and exponents were evaluated, the outcome is:

$$\frac{L_A}{d_t} = 4.91902 \left| \frac{d_p}{d_t} \right|^{0.10058} \left| \frac{w_s}{w_g} \right|^{-0.11691} \left| \frac{u_g \mu_g}{d_t^{\,2} g \rho_g} \right|^{0.28574} \left| \frac{\rho_p}{\rho_g} \right|^{0.42484} \quad (2)$$

L_A values, experimental (Table 5) and calculated from the model equation, are plotted in Fig. 7 and a reasonably good agreement between the two, especially in the trend is observed. A good concurrence in the magnitudes can also be noticed at most of the data points.

Table 5. Values of acceleration length (L_A) obtained from experiments.

System	Particle Size, d_P, µm	Particle Density, ρ_p, kg/m^3	Gas Velocity, u_g, m/s	Solid Feed Rate, w_s, kg/s	Gas Feed Rate, w_g, kg/s	Acceleration Length, L_A from $\Delta P/\Delta L$ vs. L Plot
Limestone-Gas	98	2730	6.6	0.018	0.015	0.61
Limestone-Gas	98	2730	8.1	0.018	0.018	0.82
Limestone-Gas	98	2730	14.6	0.018	0.033	1.23
Limestone-Gas	98	2730	15.3	0.013	0.035	0.99
Limestone-Gas	240	2730	15.3	0.013	0.035	1.08
Limestone-Gas	480	2730	15.3	0.013	0.035	1.24
Limestone-Gas	98	2730	10.64	0.011	0.024	0.88
Limestone-Gas	98	2730	10.64	0.018	0.024	0.81
Limestone-Gas	98	2730	10.64	0.041	0.024	0.78
Limestone-Gas	480	2730	14.67	0.032	0.034	1.21
Limestone-Gas	480	2730	14.67	0.032	0.034	0.98

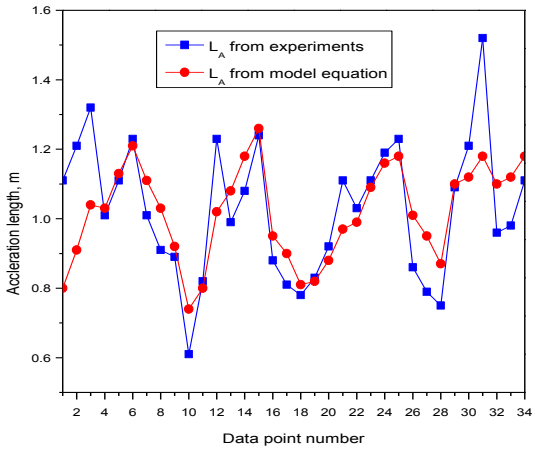

Fig. 7. Acceleration length (L_A) obtained from experiments and model equation.

3.2. Heat transfer studies

In many industrial processes fluid-to-particle heat transfer is frequently encountered. Because of its immense potential for industrial applications, the phenomenon has

rather been extensively studied. Correlations proposed for predicting the heat transfer coefficient are quite varied in nature. Reynolds number and Froude number have been chosen as the dynamic groups, the physical properties being related in Federov number, Archimedes number, etc. The film coefficient of heat transfer was expressed either in the form of Nusselt number or j_H. In many cases, the system geometry played an important role. Prandtl number appeared to have no significant effect because the power of the Prandtl number is nearly zero.

3.2.1. Variation of gas and solid temperatures for limestone-gas system

Variation of solid and gas temperatures along the riser height was provided in Tables 6 and 7 at different solid feed rates (0.0099 to 0.0411 kg/s), the temperature of gas decreases and temperature of solid increases from bottom to top of the riser. These temperatures were used to calculate the rate of heat transfer and heat transfer coefficients.

Table 6. Variation of gas and solid temperatures with solid feed rate. (Particle size: 98 μm; Gas flow rate: 0.0311 kg/s)

Riser Height (m)	Solid Feed Rate (kg/s)							
	0.0101		0.0201		0.0301		0.0411	
	t_g	t_p	t_g	t_p	t_g	t_p	t_g	t_p
0.0	255	34	257	35	252	35	251	38
0.2	234	111	228	91	220	69	217	64
0.4	225	137	216	101	207	78	198	71
0.6	219	150	206	111	194	84	187	77
0.8	211	167	202	126	189	92	179	84
1.0	207	178	197	130	182	98	174	90
1.2	203	180	194	132	178	102	168	92
1.4	200	182	196	135	171	104	168	94
1.6	196	183	192	137	169	107	164	96
1.8	194	185	181	139	168	110	159	98
2.0	192	186	175	141	166	112	152	100

t_g: Gas Temperature in ^oC t_p: Solid Temperature in ^oC

Table 7. Variation of gas and solid temperatures with solid feed rate. (Average particle size: 98 μm; Gas flow rate: 0.0273 kg/s)

Riser Height (m)	Solid Feed Rate (kg/s)							
	0.0099		0.0181		0.0281		0.0371	
	t_g	t_p	t_g	t_p	t_g	t_p	t_g	t_p
0.0	186	34	188	36	184	33	186	37
0.2	158	83	164	65	160	59	154	51
0.4	154	94	151	72	148	66	141	58
0.6	151	99	142	80	136	70	137	64
0.8	153	108	141	88	134	76	130	72
1.0	151	114	137	95	128	80	124	77
1.2	147	121	136	97	124	88	120	84
1.4	146	124	134	99	119	94	114	90
1.6	143	126	130	101	114	97	110	96
1.8	140	128	128	103	111	100	107	98
2.0	139	130	126	105	110	101	106	99

3.2.2. Correlation of Nusselt number

To fit the experimental data, a correlation of the following type has been developed, which is valid for higher ranges of solid concentration.

$$\mathrm{Nu} = a\,\mathrm{Re}_P^{\ b}\,\mathrm{Pr}^c \tag{3}$$

$$\frac{hd_t}{K} = a\left(\frac{d_P v\rho}{\mu}\right)^b\left(\frac{C_P\mu}{K}\right)^c \tag{4}$$

Through regression analysis of the experimental data, the constant a and exponents b and c were evaluated, given in Eq. (5).

$$\mathrm{Nu} = 0.40969(\mathrm{Re}_P)^{0.99953}(\mathrm{Pr})^{0.03569} \tag{5}$$

where $10 \le \mathrm{Nu} \le 200$, $0.7052 \le \mathrm{Pr} \le 0.7072$, $20 \le \mathrm{Re_p} \le 250$

Nusselt number values, experimental and calculated from the model equation, are plotted in Fig. 8 and a reasonably good agreement between the two, especially in the trend is observed.

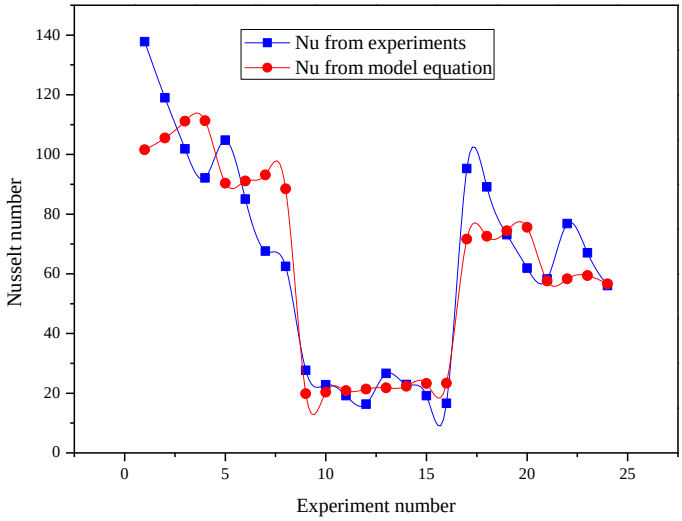

Fig. 8. Comparison of Nusselt number obtained from experiments and empirical model.

4. Conclusions

The following conclusions were made from the experimental results of hydrodynamics and heat transfer aspects of a laboratory riser system using chalcopyrite particles:

- Variation of acceleration length with different parameters such as gas velocity, particle size and solid loading ratio has been deduced for limestone.
- Variation of acceleration length with material density has been deduced for sand, limestone and chalcopyrite.

- An empirical correlation is developed for acceleration length using regression analysis:

$$\frac{L_A}{d_t} = 4.91902\left|\frac{d_p}{d_t}\right|^{0.10058}\left|\frac{w_s}{w_g}\right|^{-0.11691}\left|\frac{u_g\mu_g}{d_t^{\,2}g\rho_g}\right|^{0.28574}\left|\frac{\rho_p}{\rho_g}\right|^{0.42484}$$

- Statistical analysis between the experimental and calculated (using correlation) values of the acceleration length is also made and a correlation coefficient of 0.95 is obtained.
- Exhaustive heat transfer studies were made in hot model by varying particle size, solid flow rate and gas velocities.
- Instantaneous gas and particle temperature profiles were obtained experimentally.
- An empirical correlation is developed for Nusselt number using regression analysis, $\mathrm{Nu} = 0.40969(\mathrm{Re}_P)^{0.99953}(\mathrm{Pr})^{0.03569}$.
- Statistical analysis between the experimental and calculated (using correlation) values of the Nusselt number is also made and a correlation coefficient of 0.93 is obtained.

References

1. Abdulkadir, M.; Hernandez-Perez, V.; Lowndes, I.S.; Azzopardi, B.J.; and Dzomeku, S. (2014). Experimental study of the hydrodynamic behavior of slug flow in a vertical riser. *Chemical Engineering Science*, 106, 60-75.
2. Dutta, A.; Constales, D.; and Heynderickx, G. (2012). Applying the direct quadrature method of moments to improve multiphase FCC riser reactor simulation. *Chemical Engineering Science*, 83, 93-109.
3. Das, M.; Saha, R.K.; and Meikap, B.C. (2010). Hydrodynamic characteristics of dry beneficiation of iron ore and coal in a fast fluidized bed. *World Academy of Science, Engineering and Technology*, 4(5), 321-324.
4. Nazif, H.R.; and Tabrizi, H.B. (2013). Development of boundary transfer method in simulation of gas-solid turbulent flow of a riser. *Applied Mathematical Modelling*, 37(4), 2445-2459.
5. Zhu, J. (2001). An experimental investigation on solid acceleration length in the riser of a long circulating fluidized bed. *Chinese Journal of Chemical Engineering*, 9(1), 70-76.
6. Feng, J.; Dong, H.; Gao; J., Liu, J.; and Liang, K. (2016). Experimental study of gas-solid overall heat transfer coefficient in vertical tank for sinter waste heat recovery. *Applied Thermal Engineering*, 95, 136-142.
7. Kalita, P.; Saha, U.K.; and Mahanta, P. (2013). Parametric study on the hydrodynamics and heat transfer along the riser of a pressurized circulating fluidized bed unit. *Experimental Thermal and Fluid Science*, 44, 620-630.
8. Khalifa, M.G.; Zohir, A.E.; and Wanis, M.M. (2006). Study of the main energetic parameters in the rotary kiln. *Proceeedings of the First Scientific Environmental Conference. Zagazig University, Egypt*, 171-194.

9. Li, S.; Wu, J.Y.; Wang, R.Z.; and Huangfu, Y. (2007). Study of heat and mass transfer in integrated thermal management controller (ITMC) employed in waste heat recovery application. *Energy Conversion and Management*, 48(12), 3074-3083.
10. Liyun, Z.; Yiping, F.; Zhenbo, W.; and Chunxi, L. (2016). Comparative study of hydrodynamic and mixing behaviors in different pre-lifting schemes for an FCC riser. *Powder Technology*, 301, 557-567.
11. Wong, R.; Pugsley, T.; and Berrut, F. (1992). Modeling the axial voidage profiles and flow structure in risers of circulating fluidized beds. *Chemical Engineering Science*, 47(9), 2301-2306.
12. Yong, C.; Faqi, Z.; and Yaodong, W. (2015). Experimental analysis of the solids acceleration region in a circulating fluidised bed riser. *Indian Chemical Engineer*, 57(2), 136-146.